Mechanistic Approach for Fiber-Reinforced Flexible Pavements

Nilanchala Swain[1]; Barsa Priyadarshini Sahoo[2]; Bipash Mohanty[3] ;Dr. S. C. Mishra[4]

[1] Assistant Professor, Dept. of Civil Engineering, Aryan Institute of Engineering and Technology Bhubaneswar

[2] Assistant Professor, Dept. of Civil Engineering, Raajdhani Engineering College, Bhubaneswar

[3]Assistant Professor, Dept. of Civil Engineering,Capital Engineering College(CEC),Bhubaneswar

[4]Professor Dept. of Civil Engineering, NM Institute Of Engineering & Technology Bhubaneswar

Abstract: The present study investigates the benefits of reinforcing the subgrade soils in flexible pavements. Three types of Soils A, B, and C, and one type of polypropylene fiber having aspect ratios of 50, 84, and 100 were selected. The California bearing ratio (CBR) and unconfined compressive strength tests were conducted on unreinforced and reinforced soils. The optimum quantity of fibers was decided based on CBR, modulus of elasticity (E_i) and failure stress. The static triaxial tests were conducted on unreinforced and reinforced soilsas well as on other pavement layers at a confining pressure of 40 kPa. These stress-strain data were used as input parameters for evaluating the vertical compressive strain at the top of subgrade soils using elastoplastic finite-element analysis. This vertical compressive strain at the top of unreinforced and reinforced subgrade soils was used for estimating the improvement in service life of the pavement or reduction in thicknesses of different layers for the same service life due to reinforcing the subgrade soils.

Keywards: Fiber reinforced materials; Flexible pavements; Mechanical properties; California bearing ratio.

Introduction

The escalating cost of materials and energy and lack of resources available have motivated highway engineers to explore new alternatives in building new roads and rehabilitating the existing ones. Reinforcing the subgrade soils with short fibers is one such alternative. Recently, synthetic materials like geotextiles, geogrid, and fibers have evoked considerable interest among both highway engineers and manufacturers for using these materials as reinforcing materials in flexible pavements. However, absence of a well-documented design procedure for reinforced flexible pavements has resulted in low confidence in highway engineers while using these materials. Reinforcing the subgrade soils with short fibers appears to have the greatest potential for successful application in the design of flexible pavements. These benefits can be realized by extending the service life of the pavement or reduction in subbase or base thickness. The necessary modification can be brought about in the existing design procedure by using new materials for the pavement construction. A finite-element model of the pavement-layered structure provides the most modern technology and sophisticated characterization of materials that can be easily accommodated in the analysis. Such a realistic geometry and characterization accomplished through the use of a finite-element solution improves the ability to reliably predict the pavement response, which leads to a better design methodology.

The primary objective of the present study is to evaluate the benefits in terms of traffic benefit ratio (TBR) and layer thickness reduction (LTR) due to reinforcing the subgrade soils with short polypropylene fiber.

Earlier Work

Lawton and Fox (1992) noted that sand reinforced with multi-oriented geosynthetics results in to the highest ultimate strength in terms of its California bearing ratio (CBR). Tingle et al. (2002) observed that geo-fiber stabilization of medium sand improves the CBR by about sixfold. This improvement was attributed to the confinement of sand particles by discrete fibers. Murugesan (2004) examined the CBR of the subgrade soil reinforced with coconut, jute, and nylon fibers at various percentages and reported an overall increase in CBR by 60% due to fiber reinforcement and that an optimum percentage of fiber content lies between 0.5 and 0.6.

Al-Wahab and Al-Ourna (1995) observed that the fiber reinforcement significantly improves the peak and postpeak strength, ductility, toughness, and energy absorption capacity of a soil. Fibers ranging from 0 to 5% and fiber length from 6.35 to 50.8 mm were used to decide the optimum fiber content. Kumar et al. (1999) reported that the optimum quantity of fibers lies between 0.3 and 0.4%. Al-Wahab and Heckel (1995) pointed out that cohesive soil reinforced with just 1% fiber content increases the unconfined compressive strength, ductility, toughness, and the energy absorption capacity. Gray (1990) examined triaxial compression test results of five types of sand and five types of fibers to understand the static response of sand reinforced with fibers. The results indicated that uniform rounded sand exhibits linear behavior while well-graded and angular sands exhibit bilinear behavior. Ranjan et al. (1996) examined the data of more than 500 triaxial tests conducted on different types of sand reinforced with natural and synthetic fibers and observed that the stress-strain behavior of fiber-reinforced sand was much different from that of unrein-

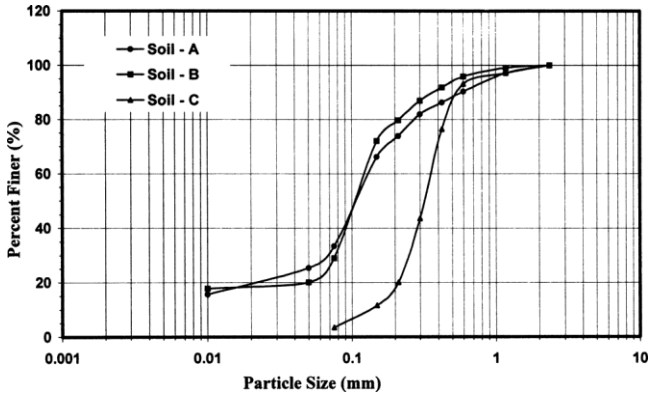

Fig. 1. Particle size distribution of soils

forced sand. Unreinforced sand attained the peak stress at about 10% of axial strain, whereas reinforced sand specimens did not fail even up to 20% of axial strain. Michalowski and Cermak (2003) observed that small a amount of polyamide fibers increases the failure stress of the composite. The effect was associated with a drop in the value of initial stiffness and increase in the strain at failure.

Experimental Program

Material Selection

Three types of soils, referred to as Soils A, B, and C in this paper, and one type of fiber were selected for the present study. The grain size distribution curves obtained for these soils are shown in Fig. 1. The index properties: liquid limit, plastic limit and plasticity index, and other important soil properties as per AASHTO and United States soil classification systems are presented in Table 1. Soil A is clay of low compressibility (A-6), Soil B is silt of low compressibility (A-2-4), and Soil C is silty sand (A-3). The polypropylene fiber, with a diameter of 0.3 mm, was selected for reinforcing the soils. The fibers were cut into pieces of 15, 25, and 30 mm length giving the value of aspect ratio as 50, 84, and 100, respectively. The fibers were used in different percentages of 0.75, 1.5, 2.25, and 3 by dry weight of soil.

Testing Program

CBR Tests

A standard Proctor's test was carried out on unreinforced and reinforced soils at different fiber contents and aspect ratios to obtain the maximum dry density (MDD) and the optimum moisture content (OMC). The dry weights of soil and fibers for each aspect ratio were calculated using the Proctor's density and the volume of CBR mold. A total of 39 samples were tested for three types of soils at different fiber contents and aspect ratios after soaking the samples in water for 4 days. It was observed that the CBR at 5 mm penetration was consistently higher than that at 2.5 mm penetration for reinforced samples. The values of CBR for different aspect ratios, fiber contents, and percent increase in CBR with respect to unreinforced soils are presented in Table 2. As may be seen, the CBR increases substantially due to reinforcement. The increase is sensitive to both fiber content and aspect ratio. Although the CBR of a soil continued to increase with the increase in fiber content and aspect ratio, mixing of fibers in soil beyond a fiber content of 1.5% was extremely difficult and initial concavity was observed in the load-penetration curve for all specimens. The CBR of a soil is correlated with fiber content (FC) and aspect ratio (AR) by following linear equations:

for Soil A

$$\underset{}{\text{CBR}} = \underset{(3.49)}{-2.286} + \underset{(4.27)}{0.0388}(\text{AR}) + \underset{(5.19)}{1.17}(\text{FC}) \quad (1)$$

for Soil B

$$\underset{}{\text{CBR}} = \underset{(2.48)}{-0.353} + \underset{(3.47)}{0.0354}(\text{AR}) + \underset{(5.01)}{1.27}(\text{FC}) \quad (2)$$

for Soil C

$$\underset{}{\text{CBR}} = \underset{(5.65)}{9.147} + \underset{(2.29)}{0.0492}(\text{AR}) + \underset{(2.43)}{1.35}(\text{FC}) \quad (3)$$

The values given in parentheses are the *t* values which are greater than the tabulated *t* value of 2.26 at 9 degrees of freedom and 5% level of significance.

Unconfined Compression Strength Tests

Unconfined compression and triaxial compression test specimens were prepared in a split mold of 100 mm diameter and 200 mm height. The tests were conducted on unreinforced and reinforced soils at different fiber contents and aspect ratios and the values of modulus of elasticity and failure stresses were evaluated. A total

Table 1. Physical Properties of Soils A, B, and C Used in Present Study

Property	Soil A	Soil B	Soil C
Dry density (kN/m^3)	16.9	17.70	19.3
Optimum moisture content (%)	17.00	14.00	11.40
Specific gravity	2.16	2.21	2.40
Coefficient of uniformity	—	—	2.64
Coefficient of curvature	—	—	1.21
D_{50} (mm)	0.11	0.11	0.33
Liquid limit (%)	34.00	28.00	—
Plastic limit (%)	22.00	19.30	NP
Plasticity index	12	8	—
Unified soil classification	CL	ML	SM
Classification as per AASHTO	A-6	A-2-4	A-3
Typical name	Clay of low compressibility	Silt of low compressibility	Silty sand

Table 2. CBR Values for Unreinforced and Reinforced Soils

Aspect ratio (l/d)	Fiber Content (%)	Soil A CBR (Soil A) (%)	Soil A Increase in CBR (%)	Soil B CBR (Soil B) (%)	Soil B Increase in CBR (%)	Soil C CBR (Soil C) (%)	Soil C Increase in CBR (%)
—	0.00	1.16	—	1.95	—	6.20	—
	0.75	1.19	2.58	2.60	33.33	11.93	92.42
50	1.50	1.61	38.80	3.11	59.48	14.00	125.80
	2.25	2.53	118.10	4.95	153.84	14.60	135.48
	3.00	2.58	122.40	5.12	162.56	16.00	158.06
	0.75	1.21	4.31	2.67	36.92	14.58	135.16
84	1.50	1.63	40.51	3.63	86.15	18.03	190.80
	2.25	3.40	193.10	5.93	204.10	16.03	158.54
	3.00	4.80	313.80	5.97	206.15	14.80	138.70
	0.75	2.23	92.24	4.15	112.82	12.55	102.42
100	1.50	4.33	273.27	6.42	229.23	16.97	173.71
	2.25	4.67	302.58	6.50	233.33	18.38	196.45
	3.00	5.02	332.75	6.45	230.76	18.41	196.93

of 39 samples were tested and the test data analyzed. The stress-strain curves of soil are nonlinear since the onset of loading. So, the modulus of elasticity was calculated corresponding to the initial tangent to the stress-strain curves. Typical stress-strain curves for unreinforced and reinforced soils are given in Fig. 2 for different fiber contents. A reduction in initial stiffness of the reinforced soil was observed when the fiber content was increased beyond 1.5%. This drop in initial stiffness may be due to the change in fabric of the soil produced by the fibers. The fibers produce nonuniform distribution of voids preventing dense packing. It results in lowering the stiffness at initial stages of loading.

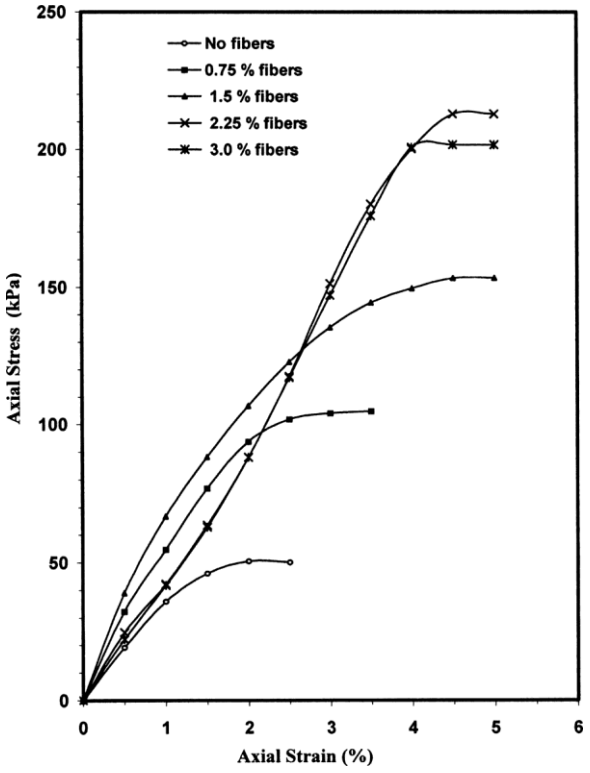

Fig. 2. Typical stress-strain curves for Soil A at aspect ratio of 100

Therefore, initial correction was applied while calculating the elastic modulus of soils reinforced with fiber content exceeding 1.5%. The failure stress and corresponding strain were found to improve with increase in fiber content. The values of modulus of elasticity (E_i), failure stress ($(\sigma_1)_f$), and corresponding strains (ε_f) observed in the case of unreinforced and reinforced soils are presented in Table 3 for different fiber contents and aspect ratios. A comparison of Tables 2 and 3 indicates that E_i values are not as sensitive to fiber reinforcement as the CBR values. This is attributed to the nature of the two tests. The CBR is a penetration test and an indirect measure of shear strength of a soil while E is obtained from a compression test. Fiber reinforcement is more effective in shearing than in compression and therefore more improvement in CBR is observed due to fiber reinforcement.

Optimum Quantity of Fibers

Optimum quantity of fibers was determined based on CBR value, modulus of elasticity (E_i), and the failure stress $(\sigma_1)_f$ of fiber-reinforced soils as explained earlier. Although the CBR of reinforced soils continued to increase with both fiber content and aspect ratio, mixing was extremely difficult beyond the fiber content of 1.5%. Also, the initial concavity was observed in load-penetration curves for all the specimens reinforced beyond 1.5% fiber content. Therefore, 1.5% fiber content and an aspect ratio of 100 were considered optimum for Soils A and B, whereas 1.5% fiber content with an aspect ratio of 84 was found to be optimum for Soil C. The CBR of Soils A, B, and C was found to be 1.16, 1.95, and 6.20%, respectively. These values increased to 4.33, 6.42, and 18.03%, respectively, due to reinforcing the soil at optimum fiber content.

The parameters like modulus of elasticity and failure stress were used as a second judgment factor for deciding the optimum fiber content. The stress-strain curves of unreinforced and reinforced soils display the concavity in the initial portion of stress-strain curves for the specimens reinforced with more than 1.5% fiber content. Also, the failure stress for specimens reinforced with 3% fiber content sometimes shows lesser values than those for 2.25% fiber content. Hence 1.5% fiber content and an aspect ratio of 100 were considered as an optimum quantity for Soils A and B, whereas 1.5% fiber content with an aspect ratio of 84 was

Table 3. Modulus of Elasticity, Failure Stresses, and Strains for Different Soils

Aspect ratio (l/d)	Fiber content (%)	Modulus of elasticity, E value (MPa)			Failure stress $(\sigma_1)_f$ (kPa)			Failure strain (ε_f) (%)		
		Soil A	Soil B	Soil C	Soil A	Soil B	Soil C	Soil A	Soil B	Soil C
—	0.00	3.834	4.836	5.572	50.60	60.14	62.60	2.00	2.00	2.50
	0.75	5.140	5.631	6.160	83.65	88.16	99.145	2.50	3.00	3.00
50	1.50	6.072	6.500	7.218	94.88	108.25	118.75	3.50	3.50	4.00
	2.25	6.012	6.992	6.520	96.50	129.12	139.78	3.50	3.50	4.00
	3.00	5.060	5.796	6.600	107.10	130.78	160.78	4.50	3.50	4.00
	0.75	5.672	7.080	6.614	80.20	97.10	116.49	3.00	3.25	4.00
84	1.50	6.738	7.854	9.712	110.00	146.55	187.78	3.50	3.50	4.50
	2.25	6.538	6.730	6.552	122.80	173.40	201.40	5.00	6.00	5.00
	3.00	6.052	6.065	6.065	132.78	210.40	204.36	4.50	6.25	—
	0.75	6.072	8.220	7.987	91.41	122.00	120.78	3.00	3.00	4.00
100	1.50	7.160	9.056	8.512	153.40	180.75	175.16	4.50	4.25	4.50
	2.25	6.500	9.020	6.167	222.30	224.00	205.78	5.00	5.00	5.00
	3.00	6.500	8.075	6.018	200.80	228.70	200.78	4.00	6.50	—

considered as an optimum quantity for Soil C. The values of CBR, modulus of elasticity (E value), and the failure stress $(\sigma_1)_f$ of Soils A, B, and C at the optimum fiber content are given in Table 4.

Finite-Element Modeling

A two-dimensional (2D) axisymetric, elastoplastic finite-element analysis of the mechanistic pavement model resting on unreinforced and reinforced subgrade soils was carried out by using ANSYS software in order to quantify the benefits of reinforcement. The values of deformations, strains, the stress at the top of subgrade were captured from each computer run. Also, a parametric study was carried out to investigate the effect on vertical compressive strains developed at the top of the subgrade due to change in the thickness of the subbase or the granular base or dense bituminous macadam (DBM).

Mechanistic Response Model

The pavement section was modeled as an axisymmetric solid to obtain mechanistically the layered pavement response due to traffic loading and to investigate the benefits of reinforcing the subgrade soil in the flexible pavement design. The thickness of each layer above the subgrade soils was decided based on CBR of subgrade soils for an assumed design traffic intensity of 150 million standard axle (msa) as per Indian code of practice, IRC 37-2001. Table 5 gives the values of thickness of various layers and the total thickness of the pavement.

Indian Roads Congress (IRC 2001) recommends that if the CBR value of subgrade soil is less than 2%, the design should be based on CBR of 2% and a capping layer of sand of 150 mm thickness should be provided in addition to the subbase thickness. Hence, a capping layer of 150 mm has been provided in addition to the subbase thickness for Soils A and B.

Table 4. Properties of Soils at Optimum Fiber Content

Materials		CBR value (%)	E value (MPa)	Failure stress $(\sigma_1)_f$ (kPa)
Soil A	Unreinforced	1.16	3.834	50.60
	Reinforced	4.33	7.160	153.40
Soil B	Unreinforced	1.95	4.836	60.14
	Reinforced	6.42	9.056	180.75
Soil C	Unreinforced	6.20	5.572	62.60
	Reinforced	18.03	9.712	187.78

Dimensions of Model and Loading

Dimensions of finite element should be sufficiently large so that constraints imposed at the boundaries have very little influence on the stress distribution in the system. Helwany et al. (1998) discretized a three layer pavement system with a right boundary at a distance of about eight times the loaded radius and adopted a uniform tyre pressure of 550 kPa acting on a circular contact area with a radius of 160 mm. Kwon et al. (2005) considered 76 mm thick asphalt concrete layer and 254 mm thick unbounded aggregate base course resting on the subgrade soil. A uniform tyre pressure of 828 kPa was considered to simulate an overloaded tyre-pavement loading which was applied over a circular area with a radius of 102 mm and eight noded structural elements were used to define all the layers in finite-element analysis.

In the present study, the right boundary was placed at a distance of 1,100 mm from the outer edge of loaded area, which is more than seven times the radius of the applied load of 150 mm. Eight noded structural elements were used for discretization of layers in the flexible pavement. A uniform pressure of 575 kPa has been applied on a circular contact area with a radius of 150 mm as shown in Fig. 3. This uniform pressure will be caused by a single axle wheel load of 40.8 kN (4,080 kg).

Boundary Conditions

For application of a finite-element model in the pavement analysis, a five-layered system of infinite extent has been reduced to a system having finite dimensions. Fig. 3 shows a typical 2D axisymmetric finite-element model of the pavement resting on

Table 5. Thickness of Each Layer for Traffic Intensity of 150 msa (IRC 37-2001)

Subgrade soil	CBR (%)	Subgrade (mm)	Subbase (mm)	Base (mm)	DBM (mm)	BC (mm)	Total thickness (mm)
A	1.16	500	460+150[a]	250	200	50	1,610
B	1.95	500	460+150[a]	250	200	50	1,610
C	6.20	500	300	250	150	50	1,250

[a]Caping layer as CBR is less than 2%; DBM=dense bituminous macadam; and BC=bituminous concrete.

subgrade Soil A. Roller supports were provided along the axis of symmetry to achieve the condition that both the shear stresses and radial displacements are equal to zero. Similarly, the roller supports were provided along the right boundary which was placed sufficiently far away from the loaded area so as to have a negligible deflection in the radial direction. At the bottom boundary, roller supports were provided, permitting free movement in the radial direction and a restraint to any movement in the vertical direction.

Mixed Incremental-Iterative Algorithm for Nonlinear Analysis

This algorithm combines the advantages of both incremental and iterative schemes. External load is applied incrementally and after each load increment, successive iterations are performed to achieve equilibrium. In general, for a jth load increment, the state of deformation, stress and strain at the end of $(j-1)$th load increment is known, i.e., $\{\delta\}^{j-1}, \{\varepsilon\}^{j-1}, \{\sigma\}^{j-1}$ are known. The general procedure is as follows:

1. For the first iteration of jth load increment

$$\{\Delta F\}_1^j = [K^{j-1}]\{\Delta\delta\}_1^j \tag{4a}$$

whereas for any ith iteration, the force-displacement relation is given by

$$\{\psi\}_{i-1}^j = [K^{j-1}]\{\Delta\delta\}_i^j \tag{4b}$$

where $[K^{j-1}]$ =constant stiffness matrix obtained from the state of stress and strain attained at the end of the previous, i.e., $(j-1)$th load increment. Eq. (4*b*) can be solved for obtaining incremental displacements of the ith iteration and these could be used to obtain incremental strains and stresses as

$$\{\Delta\varepsilon\}_i^j = [B]\{\Delta\delta\}_i^j \tag{5a}$$

$$\{\Delta\sigma\}_i^j = [D]\{\Delta\delta\}_i^j \tag{5b}$$

2. Accumulated displacements, strains, and stresses at the end of the ith iteration are obtained as

$$\{\delta\}_i^j = \{\delta\}^{j-1} + \{\Delta\delta\}_i^j \tag{6a}$$

$$\{\varepsilon\}_i^j = \{\varepsilon\}^{j-1} + \{\Delta\varepsilon\}_i^j \tag{6b}$$

$$\{\sigma\}_i^j = \{\sigma\}^{j-1} + \{\Delta\sigma\}_i^j \tag{6c}$$

3. Principal stresses and strains in the ith iteration are then computed as: $\{\sigma_p\}_i^j$ and $\{\varepsilon_p\}_i^j$ which can be used to obtain stress and strain dependent modulii as

$$E_i^j \text{ and } \nu_i^j = f(\{\sigma_p\}_i^j, \{\varepsilon_p\}_i^j) \tag{7a}$$

and

$$[D] = [D(E_i^j, \nu_i^j)] \tag{7b}$$

4. The equilibrated force vector is then given by

$$\{F_{eq}\}_i^j = \int_v [B]^T[D][B]\{\delta\}_i^j dv \tag{8}$$

and the residual force vector at the end of the ith iteration is given by

$$\{\psi\}_i^j = (\{F\}_i^j - \{F_{eq}\}_i^j) \tag{9}$$

Check for convergence is then applied on this force residual as

$$\frac{[\{\psi_i^j\}^T\{\psi_i^j\}]^{0.5}}{[\{F_i^j\}^T\{F_i^j\}]^{0.5}} \times 100 \text{ “ tolerance limit} \tag{10}$$

Equilibrium and therefore the convergence for the jth load increment is considered to have been achieved when this force residual is below a certain tolerance level, otherwise iterations are continued until the above criterion is satisfied. Once the convergence is achieved, the next load increment, ΔF_1^{j+1}, is applied and the process is repeated until the final load level is reached. In this

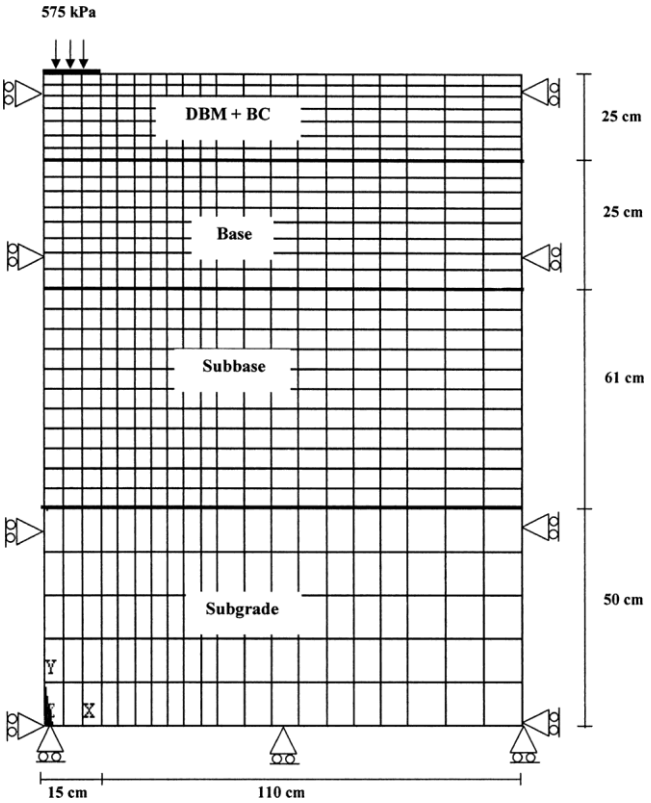

Fig. 3. Finite-element discretization of pavement section for Soil A

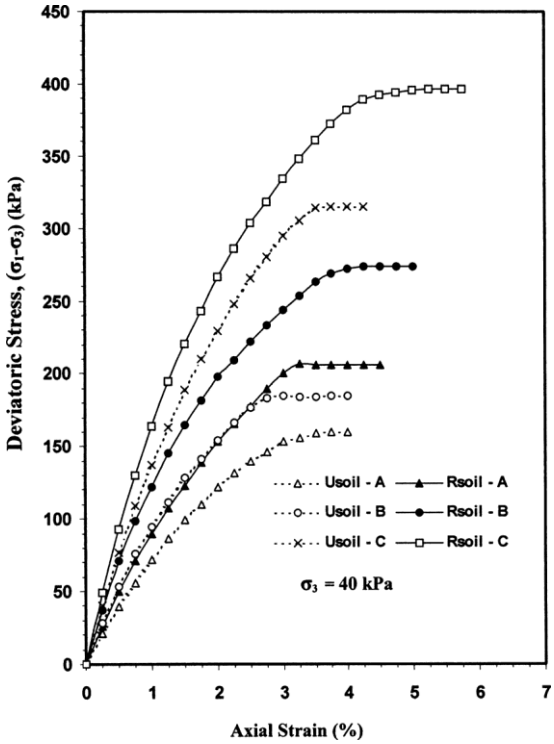

Fig. 4. Deviator stress versus axial strain curves for unreinforced and reinforced subgrade soils at confining pressure of 40 kPa

method, equilibrium can be achieved at the end of every load increment. It makes use of a variable stiffness matrix for each new load increment and maintains a constant stiffness matrix within a given load increment so as to achieve convergence and therefore the equilibrium iteratively.

Input Data for Finite-Element Modeling

The finite-element (FE) analysis of the pavement system was carried out by using the standard package ANSYS, employing the multilinear-isotropic elasto-plastic hardening model which defines the constitutive relationship of the materials involved. Properties of different layers required for carrying out the FE analysis are the modulus of elasticity, Poisson ratio, and the stress-strain data. It should be noted that the initial tangent modulus is needed only to initialize the iterative procedure and actual cumulative stress-strain data generated up to the end of a particular load increment are used in the analysis for the subsequent load increment. Chandra and Mehndiratta (2002) reported that confinement in the pavement due to shoulders and surrounding soils is in the range of 26 – 40 kPa. Hence, triaxial tests were conducted on unreinforced and reinforced subgrade soils as well as other pavement layers at a confining pressure of 40 kPa. Fig. 4 shows the resulting deviator stress versus axial strain curves for unreinforced and reinforced subgrade soils at a confining pressure of 40 kPa.

The specimens for subbase and base course materials were prepared as per the specifications of Ministry of Road Transport & Highways (MORTH 2001). The material required for DBM and bituminous concrete (BC) are aggregates, mineral filler (lime), and bitumen binder. Optimum binder content in triaxial specimens was decided based on Marshal stability tests which were 4.5 and 6.0% by weight of the total mix in DBM and BC mixes, respectively. The bulk density of DBM and BC specimens at this binder content was 23.00 and 23.75 kN/ m^3, respectively. The triaxial tests were conducted on all these pavement layer materials at a confining pressure of 40 kPa. The values of initial tangent modulus of all the pavement layers were estimated in the same manner as explained for subgrade soils and are presented in Table 6 along with the values of Poisson's ratio assumed for different layer materials.

Benefits of Reinforcement

A mechanistic-empirical design approach has been used in the present study to evaluate the benefits of reinforcing the subgrade soils in terms of reduction in layer thickness and extension in service life of the pavement. The proposed methodology has a better capability of characterizing different material properties and loading conditions, and has the ability to evaluate different design alternatives on an economic basis.

Two design alternatives considered in the present study are as follows:

1. The same service life for the reinforced and unreinforced pavement sections. It would lead to reduction in subbase, base, or DBM thickness and has been expressed in terms of LTR; and
2. The same pavement sections for unreinforced and reinforced subgrade. It would result in more service life of the pavement due to fiber reinforcement and has been expressed in terms of TBR.

Structural failures in a flexible pavement are of two types, namely surface cracking and rutting. Cracking is due to fatigue caused by repeated application of load in the bounded layer generated by the traffic. Rutting is developed due to accumulation of pavement deformation in various layers along the wheel path. Horizontal tensile strain developed at the bottom of the bituminous layer or the vertical compressive strains developed at the top of the subgrade, respectively, have been considered as indices of fatigue and rutting of the pavement structure. Since the scope of the present study is limited to reinforcing the subgrade soils only, rutting has been considered as a failure criterion. The IRC 37 (IRC 2001) considers a rut depth of 20 mm to be a failure criterion for flexible pavement and the rutting in Eq. (11) is used

Table 6. Values of Initial Tangent Modulii for Pavement Materials

	Subgrade soils									
	A		B		C					
Parameter	UR	*R*	UR	*R*	UR	*R*	Subbase	Base	DBM	BM
E (MPa)	7.56	10.36	11.18	14.68	16.21	20.50	70.12	99.20	269.67	403.33
Poisson's ratio	0.35	0.35	0.35	0.35	0.35	0.35	0.30	0.30	0.25	0.25

Note: UR=unreinforced; *R*=reinforced; DBM=dense bituminous macadam; and BC=bitumenous concrete.

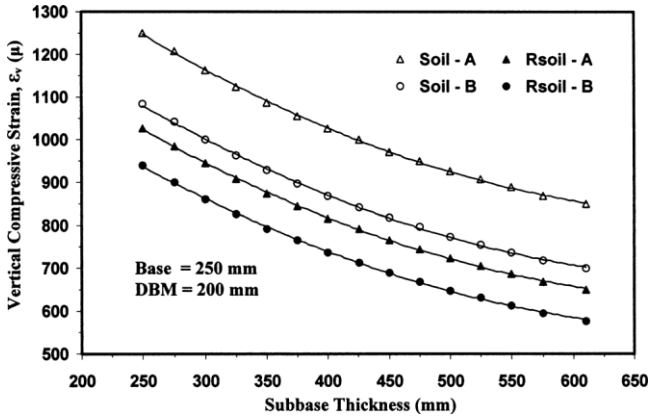

Fig. 5. Variation of vertical compressive strain at top of subgrade with subbase thickness

$$N_{20} = 4.1656^{*}10^{-8}\left(\frac{1}{\varepsilon_V}\right)^{4.5337} \tag{11}$$

where N_{20}=number of cumulative standard axles to produce a rutting of 20 mm; and ε_v =vertical compressive strain at top of subgrade.

Vertical compressive strain developed at the top of unreinforced and reinforced subgrades was captured for different thicknesses of subbase, base, and DBM. For Soils A and B, thickness of the base course of 250 mm and DBM thickness of 200 mm were maintained constant and the subbase thickness was varied. Again, keeping the subbase thickness of 610 mm and DBM thickness of 200 mm, the base thickness was varied. Similarly, DBM thickness was varied for a constant subbase of 610 mm and base thickness of 250 mm. The vertical compressive strains developed at the top of the subgrade in unreinforced and reinforced pavement sections were evaluated for all these alternatives from elasto-plastic finite-element analysis. A similar exercise was also done for Soil C. Figs. 5 and 6 show this variation of vertical compressive strain at the top of the subgrade with subbase, base, and for subgrade Soils A and B, respectively. These plots were used to study the benefits of reinforcing the subgrade soils in terms of LTR and TBR. The TBR gives the extension in the service life of pavement due to fiber reinforcement and can be written in the equation form as

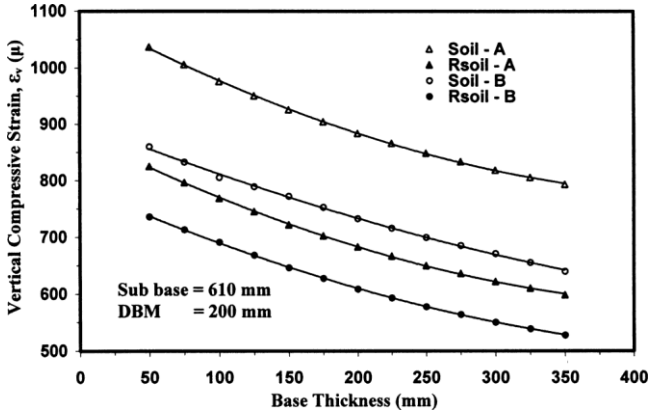

Fig. 6. Variation of vertical compressive strain at top of subgrade with base thickness

$$\text{TBR} = \frac{N_R}{N_U} \tag{12}$$

where N =number of traffic passes required for producing a pavement surface deformation (rutting) up to the allowable rut depth and expressed in mm; and R and U denote reinforced and unreinforced pavement sections.

Perkins and Edens (2002) evaluated the benefits of reinforcement in terms of LTR for the equivalent service life of the pavement. It can be defined as

$$\text{LTR} = \left(\frac{D_U - D_R}{D_U}\right) * 100 \tag{13}$$

D_U and D_R =base course thicknesses of unreinforced and reinforced pavement sections. As no separate equation is available in the literature to relate the vertical compressive strain at the top of the reinforced subgrade to the number of load repetitions necessary to produce the allowable rutting, Eq. (13) was used for both unreinforced and reinforced subgrade.

Using Eqs. (12) and (13), the benefits of fiber-reinforced subgrade soils in terms of extension in service life of a flexible pavement can be expressed as

$$\text{TBR} = \frac{N_R}{N_U} = \left(\frac{\varepsilon_{VR}}{\varepsilon_{VU}}\right)^{-B} \tag{14}$$

The vertical compressive strain, ε_v, at the top of the subgrade can be obtained through FE software and B =constant equal to 4.5337 (IRC 2001).

The results of elasto-plastic finite-element analysis presented in Figs. 5 and 6 indicate that the vertical compressive strain at the top of the subgrade in the pavement section designed with unreinforced Soil A is 848.72 μm. For a constant thickness of base and DBM, this strain level was obtained for a subbase thickness of 375 mm in the case of reinforced Soil A. Also, for a constant value of subbase and DBM thicknesses, the base thickness can be theoretically reduced to less than 50 mm for the designed strain of 848.72 μm (Fig. 6). Similarly, the designer has the option to reduce the thickness of DBM from 200 mm to less than 50 mm for the same value of design strain keeping the subbase and base thicknesses at 610 and 250 mm, respectively. The designer can consider different options of partly reducing the thickness of each layer and also finally choose the most economical section for the same service life of reinforced pavement compared to that of the unreinforced pavement.

If the pavement section is kept the same for unreinforced and reinforced subgrade soils, the vertical compressive strain reduces from 848.72 μm in the case of unreinforced subgrade to 650 μm for reinforced subgrade Soil A, giving the TBR of 3.35. It means that reinforced pavement will have a life 3.35 times that of unreinforced pavement. Similar exercises have also been done for two other types of soils. Results obtained from such a study are summarized in Table 7. These results show that for a constant thickness of base and DBM, the thickness of the subbase reduces by 38.52, 26.23, and 16.67%, respectively, for Soils A, B, and C, for almost the same service life of reinforced and unreinforced pavements. Similar options can also be exercised for base and DBM. Therefore, the flexible pavement can be designed by adopting any of the three alternatives.

The pavement can also be designed for any intermediate thickness to reduce the thicknesses of the layer as well as to gain additional benefits in terms of extension in service life of the pavement. For example, in the case of reinforced subgrade Soils

Table 7. Reinforcement Benefits in Subbase, Base, and DBM Thickness

Subgrade soils	Constant base and DBM: Subbase thickness (mm)	LTR (%)	s_{VU}/s_{VR}	TBR	Constant subbase and DBM: Base thickness (mm)	LTR (%)	s_{VU}/s_{VR}	TBR	Constant subbase and base: DBM thickness (mm)	LTR (%)	s_{VU}/s_{VR}	TBR
A	**610**	0.00	1.305	3.35	**250**	0.00	1.305	3.35	**200**	0.00	1.305	3.35
	575	5.73	1.267	2.94	**225**	10.00	1.273	2.98	**175**	12.50	1.260	2.85
	550	9.83	1.235	2.60	**200**	20.00	1.242	2.68	**150**	25.00	1.217	2.44
	525	13.93	1.202	2.31	**175**	30.00	1.208	2.36	**125**	37.50	1.169	2.04
	500	18.03	1.173	2.06	**150**	40.00	1.176	2.08	**100**	50.00	1.125	1.71
	475	22.13	1.139	1.81	**125**	50.00	1.138	1.80	**75**	62.50	1.076	1.40
	450	26.23	1.107	1.59	**100**	60.00	1.104	1.57	**50**	75.00	1.030	1.15
	425	30.32	1.073	1.38	**75**	70.00	1.064	1.33	—	—	—	—
	400	34.43	1.040	1.19	**50**	80.00	1.028	1.13	—	—	—	—
	375	38.52	1.004	1.02	—	—	—	—	—	—	—	—
B	**610**	0.00	1.211	2.38	**250**	0.00	1.211	2.38	**200**	0.00	1.211	2.38
	575	5.73	1.175	2.08	**225**	10.00	1.179	2.11	**175**	12.50	1.166	2.00
	550	9.83	1.140	1.82	**200**	20.00	1.148	1.87	**150**	25.00	1.124	1.70
	525	13.93	1.108	1.60	**175**	30.00	1.114	1.63	**125**	37.50	1.076	1.40
	500	18.03	1.079	1.41	**150**	40.00	1.082	1.43	**100**	50.00	1.033	1.16
	475	22.13	1.046	1.23	**125**	50.00	1.046	1.23	**75**	—	—	—
	450	26.23	1.015	1.07	**100**	60.00	1.012	1.06	**50**	—	—	—
C	**300**	0.00	1.158	1.94	**250**	0.00	1.158	1.94	**150**	0.00	1.158	1.94
	275	8.33	1.095	1.51	**225**	10.00	1.091	1.48	**125**	16.67	1.066	1.34
	250	16.67	1.038	1.19	**200**	20.00	1.030	1.15	**100**	33.33	1.001	1.00

Note: TBR=traffic benefit ratio; LTR=layer thickness reduction.

A or B, the thickness of the subbase can be reduced by 38.52 and 26.23%, respectively. But if the designer chooses to reduce the thickness of the subbase by 18% only, it is possible to gain additional benefits in terms of TBR of 2.06 and 1.41 for Soils A and B, respectively.

Conclusions

Two important aspects have been investigated in this study, namely, (1) the optimum quantity of fibers for a subgrade soil which gives the maximum improvement in CBR and *E* value; and (2) to evaluate the benefits of fiber-reinforced subgrade soils in flexible pavements.

The following conclusions emerged from this study:

1. CBR values of Soils A, B, and C were found to be 1.16, 1.95, and 6.20%, respectively, which increased to 4.33, 6.42, and 18.03%, respectively, due to fiber reinforcement;
2. The static modulus of neat Soils A, B, and C, uniaxial compressive strength tests, were found to be 3.824, 4.836, and 5.572 MPa, respectively. These increased to 7.16, 9.056, and 9.712 MPa, respectively, at optimum fiber content;
3. At confining pressures of 40 kPa, the initial tangent moduli of Soils A, B, and C were 7.56, 11.18, and 16.21 MPa, respectively, which increased to 10.36, 14.68, and 20.50 MPa respectively, due to reinforcement. These values are on the lower side and therefore are not recommended for the final design. However, these were used only for starting the iterative solution in the finite-element analysis and do not affect the final or overall response of the pavements;
4. If the pavement section is kept the same for unreinforced and reinforced subgrade Soils A, B, and C, the pavement resting on reinforced subgrade Soils A, B, and C gives TBR values of 3.35, 2.28, and 1.94, respectively;
5. For a constant thickness of base and DBM (as for the standard section), the thickness of the subbase reduces by 38.52, 26.23, and 16.67%, respectively, for reinforced Soils A, B, and C; and
6. The pavement resting on reinforced subgrade soils is beneficial in reducing the construction materials. Actual savings would depend upon the option exercised by the designer for reducing the thickness of an individual layer.

Notation

The following symbols are used in this paper:

AR = aspect ratio of fiber;
CBR = California bearing ratio;
D = thickness of base course layer;
$[D]$ = elasticity matrix;
E = modulus of elasticity;
E_i = initial tangent modulus;
F = force;
FC = fiber content;
f = function;
j = jth load increment;
$[K]$ = constant matrix;
LTR = layer reduction ratio;
N_{20} = number of cumulative standard axles to produce 20 mm rut depth;
R = reinforced sample;
TBR = traffic benefit ratio;
ν = strain dependent modulus;

Δ = increment;
δ = deformation;
$\{\delta\}$ = displacement vector;
ε = strain;
ε_v = vertical compressive strain at top of subgrade;
σ = stress;
$(\sigma_1)_f$ = failure stress; and
† = residual force.

Suffix

eq = equilibrated;
i = *i*th iteration;
P = principal stress or strain;
R = reinforced; and
U = unreinforced.

References

Al-Wahab, R. M., and Al-Ourna, H. H. (1995). "Fiber reinforced cohesive soil for application in compacted earth structures." *Proc., Geosynthetics—95*, Vol. II, St. Paul, Minn., 433–446.

Al-Wahab, R. M., and Heckel, G. B. (1995). "Static and dynamic strength properties of a fiber-reinforced compacted cohesive soil." *Proc., 3rd Int. Conf. on Recent Advances in Geotechnical Earthquake and Soil Dynamics*, Vol. II, St. Louis, 1065–1072.

Chandra, S., and Mehndiratta, H. C. (2002). "Effect of shoulder on life of flexible pavements." *Highway Research Bulletin 67*, Indian Roads Congress, New Delhi, India, 37–46.

Gray, D. H. (1990). "Role of woody vegetation in reinforcing soils and stabilizing slopes." *Proc., Symp. on Soil Reinforcing and Stabilizing Technique*, Sydney, Australia, 253–306.

Helwany, S., Dyer, J., and Leidy, J. (1998). "Finite element analyse of flexible pavements." *J. Transp. Eng.*, 124(5), 491–499.

Indian Roads Congress (IRC). (2001). "Guideline for the design of flexible pavements." *Indian code of practice, IRC:37*, New Delhi, India.

Kown, J., Tutumluer, E., and Kim, M. (2005). "Mechanistic analysis of geogrid base reinforcement in flexible pavements considering unbounded aggregate quality." *Proc., 5th International Conf. on Road and Airfield Pavement Technology*, Seoul, Korea, 54–63.

Kumar, R., Kanaujia, V. K., and Chandra, D. (1999). "Engineering behaviour of fiber reinforced pond ash and silty sand." *Geosynthet. Int.*, 6(6), 509–518.

Lawton, E. C., and Fox, N. S. (1992). "Field experiment on soils reinforced with multi-oriented geosynthetic inclusions." *Transportation Research Record. 1369*, Transportation Research Board, Washington, D.C., 44–53.

Michalowski, R. L., and Cermak, J. (2003). "Triaxial compression of sand reinforced with fibers." *J. Geotech. Geoenviron. Eng.*, 129(2), 125–136.

Ministry of Road Transport and Highways (MORTH). (2001). *Report of the committee on norms for maintenance of roads in India*, 4th Ed., Indian Roads Congress, New Delhi, India.

Murugesan, S. (2004). "A study of fibers as a reinforcement for subgrade of flexible pavement." *Proc., Int. Conf. on Geosynthetics and Geoenvironmental Engineering*, Mumbai, India, 163–164.

Perkins, S. W., and Edens, M. Q. (2002). "Finite element and distress models for geosynthetic-reinforced pavements." *Int. J. Pavement Eng.*, 3(4), 239–250.

Ranjan, G., Vasan, R. M., and Charan, H. D. (1996). "Probabilistic analysis of randomly distributed fiber-reinforced soil." *J. Geotech. Engrg.*, 122(6), 419–426.

Tingle, S. J., Santoni, R. L., and Webster, S. L. (2002). "Full-scale field Tests of discrete fiber-reinforced sand." *J. Transp. Eng.*, 128(1), 9–16.